

Polymer chain stiffness vs. excluded volume: A Monte Carlo study of the crossover towards the worm-like chain model

This article has been downloaded from IOPscience. Please scroll down to see the full text article.

2010 EPL 92 28003

(<http://iopscience.iop.org/0295-5075/92/2/28003>)

View [the table of contents for this issue](#), or go to the [journal homepage](#) for more

Download details:

IP Address: 134.93.131.31

The article was downloaded on 01/04/2011 at 14:02

Please note that [terms and conditions apply](#).

Polymer chain stiffness vs. excluded volume: A Monte Carlo study of the crossover towards the worm-like chain model

HSIAO-PING HSU^{1(a)}, WOLFGANG PAUL² and KURT BINDER¹

¹ *Institut für Physik, Johannes Gutenberg Universität Mainz - Staudinger Weg 7, 55099 Mainz, Germany*

² *Theoretische Physik, Martin-Luther-Universität Halle Wittenberg - von Senckendorffplatz 1, 06120 Halle, Germany*

received 31 July 2010; accepted in final form 30 September 2010

published online 15 November 2010

PACS **82.35.Lr** – Physical properties of polymers

PACS **61.46.-w** – Structure of nanoscale materials

PACS **05.10.Ln** – Monte Carlo methods

Abstract – When the local intrinsic stiffness of a polymer chain varies over a wide range, one can observe both a crossover from rigid-rod-like behavior to (almost) Gaussian random coils and a further crossover towards self-avoiding walks in good solvents. Using the pruned-enriched Rosenbluth method (PERM) to study self-avoiding walks of up to $N_b = 50000$ steps and variable flexibility, the applicability of the Kratky-Porod model is tested. Evidence for non-exponential decay of the bond-orientational correlations $\langle \cos \theta(s) \rangle$ for large distances s along the chain contour is presented, irrespective of chain stiffness. For bottle-brush polymers on the other hand, where experimentally stiffness is varied via the length of side-chains, it is shown that these cylindrical brushes (with flexible backbones) are not described by the Kratky-Porod worm-like chain model, since their persistence length is (roughly) proportional to their cross-sectional radius, for all conditions of practical interest.

Copyright © EPLA, 2010

Introduction and motivation. – One of the most basic characteristics of macromolecules with linear “chemical architecture” is chain flexibility (or lack thereof, stiffness) [1–3]. While many synthetic polymers are fully flexible, and the statistical properties of their conformations under good solvent conditions have been extensively investigated [1–5], recently also semiflexible polymers have found much interest, in particular since important biopolymers such as DNA, some proteins, rod-like viruses, or actin filaments belong to this class [6–8]. Moreover, also synthetic polymers such as polyethylene exhibit some stiffness over short distances along the chain. Particular interest in the problem of chain stiffness has arisen due to the discovery that in macromolecules with “bottle-brush architecture” [9–12] their stiffness can be varied over a wide range by changing the length and grafting density of side-chains. Since short bottle-brush polymers in solution may exhibit liquid-crystalline-type ordering [13], and their structure is very sensitive to various external stimuli, various applications for such molecules have been proposed (from building blocks of nanostructures to actuators and sensors etc. [14,15]). Also in a biological context

semiflexible macromolecules with bottle-brush architecture are found [16], and have interesting functions such as lubrication in mammalian joints [17].

While for fully flexible polymers under good solvent conditions excluded-volume interactions (loosely speaking, monomers of a polymer chain cannot “sit” on top of each other) are of central importance [1–5], the standard model to describe semiflexible chains ignores them completely [18–22]. This “standard model” is the “worm-like chain model” of Kratky and Porod [18], described by a Hamiltonian (in the continuum limit)

$$\mathcal{H} = \frac{\kappa}{2} \int_0^L dt \left(\frac{d^2 \vec{r}(t)}{dt^2} \right)^2, \quad (1)$$

where the curve $\vec{r}(t)$ describes the linear polymer of contour length L , and the parameter κ describing the bending stiffness is related to the “persistence” length ℓ_p as $\kappa = \ell_p k_B T$. For chain molecules in the absence of excluded volume, where distances between monomers that are far apart satisfy Gaussian statistics, one can show that the orientational correlation function between bond

^(a) E-mail: hsu@uni-mainz.de

vectors decays exponentially with $s = t/\ell_b$:

$$\langle \vec{a}_i \cdot \vec{a}_{i+s} \rangle = \ell_b^2 \exp(-s\ell_b/\ell_p), \quad (2)$$

where $\ell_b = |\vec{a}_i|$ is the bond length between two subsequent monomers along the chain, $\vec{a}_i = \vec{r}_i - \vec{r}_{i-1}$. Note that s is dimensionless and for a model with discrete monomers just denotes the difference in the labels $i, i+s$ of the monomers. The Kratky-Porod model then yields for the end-to-end vector \vec{R}_e of the semiflexible chain [18] ($L = N_b \ell_b$)

$$\langle R_e^2 \rangle = 2\ell_p L \left\{ 1 - \frac{\ell_p}{L} [1 - \exp(-L/\ell_p)] \right\}, \quad (3)$$

which shows the standard Gaussian behavior ($\langle R_e^2 \rangle = 2\ell_p L = 2\ell_p \ell_b N_b$) for $L \rightarrow \infty$, while for $L \ll \ell_p$ the rod-like behavior $\langle R_e^2 \rangle = L^2$ results.

However, for good solvent conditions and long enough chains eqs. (2), and (3) cannot be correct: rather we must have [23], for $N_b \rightarrow \infty$,

$$\langle \vec{a}_i \cdot \vec{a}_{i+s} \rangle \propto s^{-\beta}, \quad \beta = 2 - 2\nu \approx 0.824, \quad s^* \ll s \ll N_b \quad (4)$$

and [1–5, 24, 25]

$$\langle R_e^2 \rangle = 2\ell_{p,R} \ell_b N_b^{2\nu}, \quad (5)$$

where $\nu \approx 0.588$ [24] is the exponent describing the swelling of the chains due to excluded volume. If s is no longer much smaller than N_b , the power law eq. (4), gradually crosses over to a faster decay that depends on N_b [25]. In eq. (5), we have written a tentative generalization of the Kratky-Porod result to introduce another, effective persistence length $\ell_{p,R}$ [25]. The question that we ask in this paper hence is, how can one reconcile eq. (2) with eq. (4), as well as eq. (3) with eq. (5)? Tentatively, one might expect that for semiflexible chains eq. (2) still holds up to some characteristic, large value s^* , where then the crossover to eq. (4) takes place [26]; but such a hypothesis is by no means evident, and remains to be proven, and the value of s^* remains to be predicted. Similarly, one might expect that eq. (3) holds only for N_b up to some value N_b^* , and then a crossover to eq. (5) takes place. Using a Flory [27] argument, Netz and Andelman [28] suggested that this is the case and (implying $\nu = 3/5$)

$$N_b^* \propto (\ell_p/\ell_b)^3, \quad \ell_{p,R} \propto \ell_p^{2/5} \ell_b^{3/5}. \quad (6)$$

As expected, this result for $\ell_{p,R}$ is equivalent to the classical result [29–31] $\langle R_e^2 \rangle^{1/2} \propto \ell_b (\ell_p/\ell_b)^{1/5} N_b^{3/5}$ for semiflexible macromolecules in the limit $N_b \rightarrow \infty$.

In the present work, we hence wish to check whether such ideas about these crossovers apply, and if so, study their detailed behavior. Finally, we shall discuss whether or not these ideas have some bearing on the problem of the persistence length of bottle-brush polymers [25].

Model and simulation results. – We carried out Monte Carlo simulations of self-avoiding walks (SAWs) on the simple cubic lattice, applying an energy $\varepsilon_b(1 - \cos \theta)$ if a bond orientation differs by an angle θ relative to the preceding bond (of course, on our lattice only $\theta = 0$ or $\theta = \pm\pi/2$ are possible). Using the pruned-enriched Rosenbluth method (PERM) [32,33], the partition function of the SAWs of N_b steps with N_{bend} local bends (where $\theta = \pm\pi/2$) is written as

$$Z_{N_b, N_{\text{bend}}}(q_b) = \sum_{\text{config}} C(N_b, N_{\text{bend}}) q_b^{N_{\text{bend}}}, \quad (7)$$

where $q_b = \exp[-\varepsilon_b/k_B T]$ is the appropriate Boltzmann factor ($q_b = 1$ for ordinary SAWs). We obtained data for $C(N_b, N_{\text{bend}})$ for N_b up to $N_b = 50000$, and vary q_b over a wide range as well, $0.005 \leq q_b \leq 1.0$. In addition we have continued our simulations [25] of bottle-brush polymers using the bond fluctuation model.

Figure 1 shows that two distinct patterns of behavior emerge: for flexible or only moderately stiff chains, $0.1 \leq q_b \leq 1.0$, eq. (2) has hardly any significant regime of applicability, there are just a few discrete values for small s ($s = 1, 2, 3, \dots$) that can be fitted by eq. (2), and then pronounced deviations from a simple exponential behavior occur (fig. 1(a)). On the other hand, for large s ($s \geq 20$) the power law (eq. (4)) provides a good fit (fig. 1(b)). But it is also evident that the deviations from the power law for small s become the more pronounced the smaller q_b is. Of course, the crossover value s^* is not sharply defined, but rather the crossover is smeared out over some range in s . For small q_b ($0.005 \leq q_b \leq 0.05$) the initial exponential decay (eq. (2)) becomes better visible, fig. 1(c), and chain lengths even larger than studied by us would be needed to still clearly identify the power law for large enough s . While the exponential decay of the bond correlations (eq. (2)) works only for a restricted range of s ($s \ll s^*$) and only for very stiff chains ($q_b \ll 1$), a simple exponential decay is always found for the probability $P(n_{\text{str}})$ that sequences of n_{str} subsequent bonds without kink occur, for large n_{str} (fig. 1(d)), $P(n_{\text{str}}) \propto \exp(-n_{\text{str}}/n_p)$, where n_p then is defined as decay constant. For $q_b \ll 1$ we find that $\ell_p = n_p \ell_b$, within numerical error, and furthermore $\ell_p \propto q_b^{-1}$ holds then.

The chain linear dimensions tell a similar story (fig. 2): for flexible chains, $q_b = 1.0$ and $q_b = 0.4$, there is a monotonic increase towards the plateau that yields the value $\ell_{p,R}$ (eq. (5)), fig. 2(a). However, the resulting values for $\ell_{p,R}$ are small, unlike the case of bottle-brushes (fig. 2(b)), with one side-chain per backbone monomer, where with increasing side-chain length N rather large values of $\ell_{p,R}$ can be achieved [25]. The strong initial rise seen for small q_b in fig. 2(a), however, is indeed compelling evidence that for small q_b a rod-like behavior is found. But also for large q_b in fig. 2(a), and also in the case of the bottle-brushes (fig. 2(b)), one observes for small N_b a strong increase of $\langle R_e^2 \rangle$ with N_b , but not as strong as it would occur for rods.

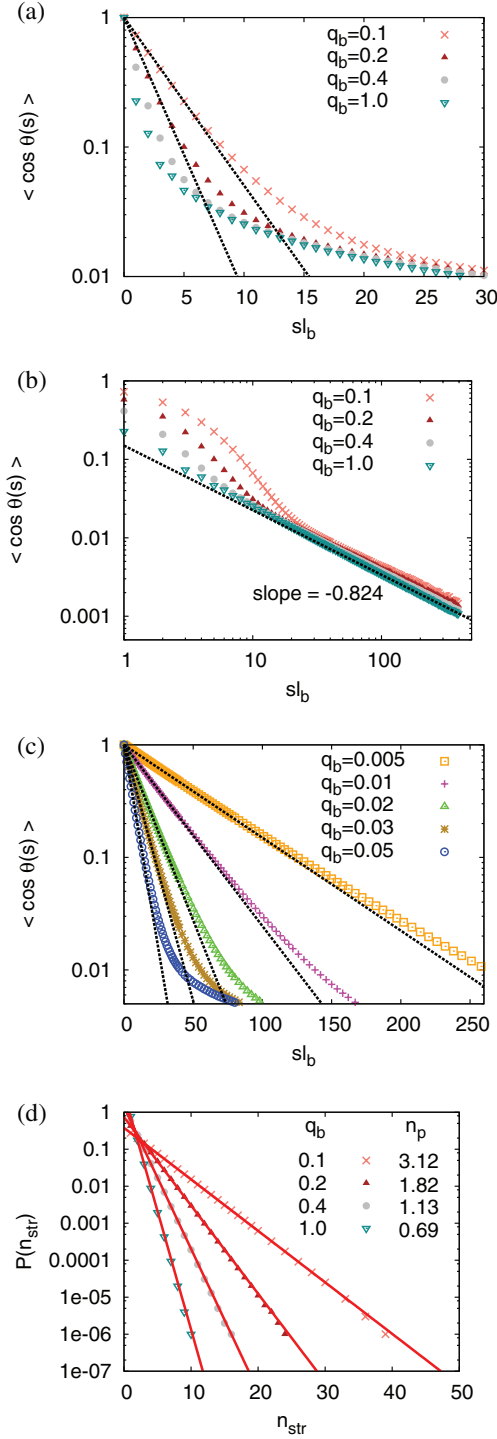


Fig. 1: (Colour on-line) Semi-log plot of the bond vector correlation function $\langle \cos \theta(s) \rangle$ *vs.* the chemical distance $\ell_b s$ along the chain (here ℓ_b is the lattice spacing which is our unit of length, $\ell_b = 1$) for $0.1 \leq q_b \leq 1.0$ (a), and for $0.005 \leq q_b \leq 0.05$ (c). Part (b) shows the same data as part (a) but on a log-log plot. The straight line indicates a fit of eq. (4) to the data for $q_b = 1$, while straight lines in (a), (c) are fits of the initial exponential decay to eq. (2). Part (d) shows the distribution function $P(n_{\text{str}})$ of straight pieces of the chain without kinks, together with fits of $P(n_{\text{str}}) \propto \exp(-n_{\text{str}}/n_p)$. $N_b = 50000$ was used throughout.

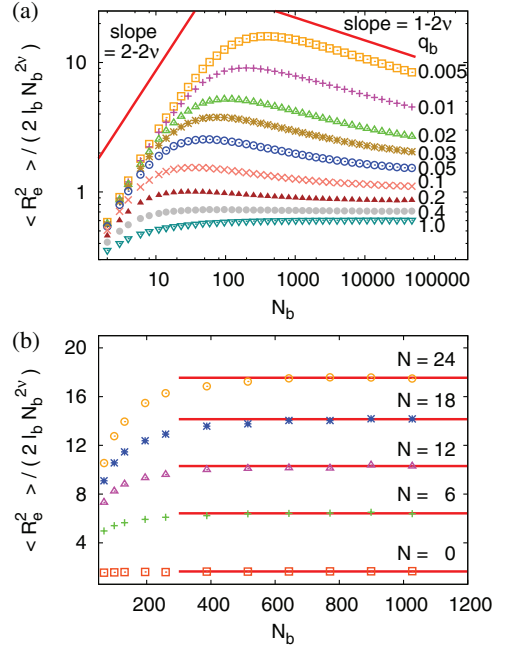


Fig. 2: (Colour on-line) Rescaled mean square end-to-end distance $\langle R_e^2 \rangle / (2\ell_b N_b^{2\nu})$ plotted against the chain length N_b for semiflexible chains with $\ell_b = 1$ and variable q_b (and hence ℓ_p) on a log-log plot (a), and analogous quantity for the backbone of a bottle-brush polymer [25], using the bond fluctuation model with excluded-volume interactions only which has $\ell_b = 2.7$ lattice spacings, and various side-chain lengths N , on a linear-linear plot (b). The slopes shown in (a) illustrate the exponents expected for rods ($\langle R_e^2 \rangle \propto N_b^2$) or Gaussian chains ($\langle R_e^2 \rangle \propto N_b$), respectively. Lengths are measured in units of the lattice spacing throughout.

Figure 3 now tests the applicability of the Kratky-Porod formula, eq. (3), to these data; extracting ℓ_p from the exponential fit of eq. (2) to the data in fig. 1(c), there is no adjustable parameter whatsoever! Here the data for $q_b \geq 0.2$ were omitted, since they clearly do not show any trace of the Gaussian behavior implied by eq. (3). For small N_b and small q_b the success of eq. (3) indeed is remarkable (fig. 3(a)), however, for large N_b we see that the data do not really settle down at the “plateau” value implied by the Gaussian behavior, but rather start to rise again, the crossover to the excluded-volume behavior sets in. Again, this crossover is spread out over about a decade in N_b (and for $q_b = 0.005$ it starts only for $N_b > 50000$!).

In experiments, information on chain stiffness of polymers, in principle, is accessible from an analysis of the static structure factor $S(|\vec{q}|)$ of single chains where \vec{q} is the scattering vector. From a “Kratky plot”, $q S(q)$ *vs.* q , one finds a position where $S(q)$ is maximal, $q_{\text{max}} \propto 1/R_{\text{gyr}}$ at small q , where R_{gyr} is the gyration radius of the polymer, and a power law $q S(q) \propto q^{-(1/\nu-1)}$ for chains exhibiting excluded-volume statistics at larger q . For very stiff chains, one would expect that this power law crosses over to the

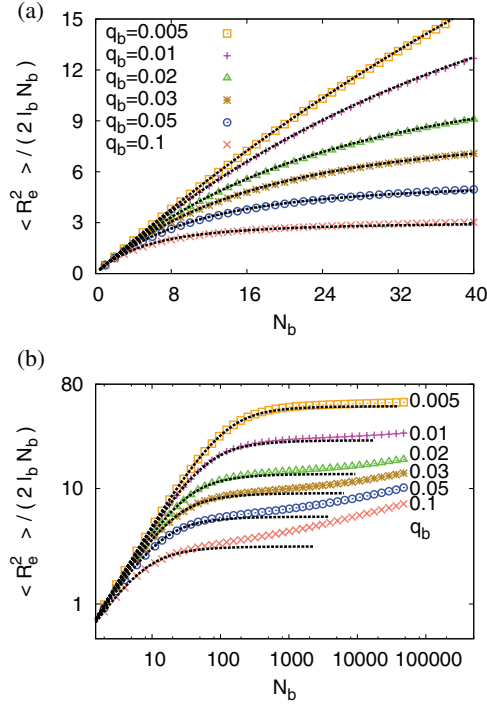


Fig. 3: (Colour on-line) Plot of $\langle R_e^2 \rangle / 2\ell_b N_b$ vs. N_b , on linear-linear scales, for $N_b \leq 40$ (a) and on log-log scales, up to $N_b = 50000$ (b), using only the data for $0.005 \leq q_b \leq 0.1$. Dotted curves refer to the discrete chain model of [21].

Gaussian behavior $qS(q) \propto q^{-1}$ at large q and ultimately a further crossover to the scattering function from straight rods, $qS(q) = \text{const}$, should occur. Figure 4(a) shows that the latter regime is only found for the stiffest chains that we could study ($q_b = 0.005$), and the onset of this so-called “Holtzer plateau” [34] in the Kratky plot is rather gradual: contrary to some suggestions [35,36], estimation of the value q^* where this onset occurs is not suited as an accurate method to extract $\ell_p (= 1/q^*)$. Figure 4(a) also shows that the expected power laws cannot be clearly identified either, because the crossover between them is too gradual. Figure 4(b) reveals that also the position q_{max} where $qS(q)$ has its maximum does not (yet) exhibit the expected power laws [28]: the reason is that for small q_b the chain length $N_b = 50000$ still is by far too short for the mean square radii $\langle R_e^2 \rangle$ (cf. fig. 2(a)) and $\langle R_{\text{gyr}}^2 \rangle$ to reach their asymptotic behavior. The smaller q_b becomes (and the larger hence ℓ_p is) the more Gaussian character of the chains do we expect for fixed $N_b = 50000$, and hence we see a gradual crossover from $q_{\text{max}} \propto \ell_p^{-1/5}$ to $q_{\text{max}} \propto \ell_p^{-1/2}$ with increasing ℓ_p on the log-log plot.

Returning now to the behavior of bottle-brush polymers (fig. 2(b)), we emphasize that pronounced local stiffness occurs there by a completely different mechanism, namely as a consequence of the local thickening of the (coarse-grained) cylindrical chains. This thickening with increasing side-chain length N is evident from the radial

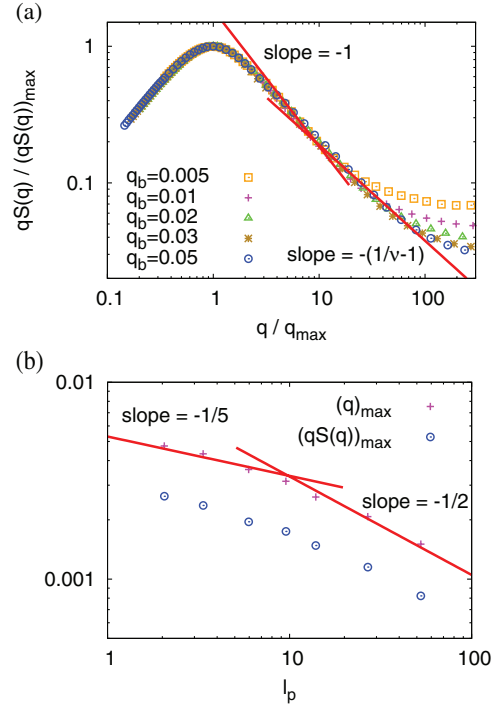


Fig. 4: (Colour on-line) (a) Rescaled Kratky plot, log-log plot of $qS(q)/[qS(q)]_{\text{max}}$ vs. q/q_{max} , for several choices of q_b as indicated. The straight lines indicate the effective exponents that occur in the regime of intermediate wave numbers q . The position q_{max} where $qS(q)$ exhibits its maximum $[qS(q)]_{\text{max}}$, and the height of this maximum is plotted in (b) as function of ℓ_p . Straight lines indicate the exponents $q_{\text{max}} \propto \ell_p^{-1/5}$ and $q_{\text{max}} \propto \ell_p^{-1/2}$ that one expects according to Netz and Andelman [28] in the excluded-volume regime and Gaussian regime, respectively. All data have been taken for $N_b = 50000$.

density distribution in the plane (locally [37]) perpendicular to its backbone (fig. 5(a)). Normalizing $\rho(r)$ in fig. 5(a) such that $N = 2\pi \int_0^\infty \rho(r)r dr$, the cross-sectional radius $R_{\text{cs}}(N)$ can be defined as $R_{\text{cs}}^2 = 2\pi \int \rho(r)r^3 dr$. We now view the bottle-brush polymer as a sequence of blobs with diameter $2R_{\text{cs}}(N)$. Figure 5(b) shows the construction. On the ordinate the values for $2R_{\text{cs}}(N)$ are indicated, and we can identify how many backbone monomers $s_{\text{blob}}(N)$ occur per blob by requiring $\Delta r(s_{\text{blob}}(N)) = 2R_{\text{cs}}(N)$. We find $s_{\text{blob}} = 6, 10, 12$ and 14 , for $N = 6, 12, 18$ and 24 , respectively. If we rescale N_b with s_{blob} , and $\langle R_{e,b}^2 \rangle$ in fig. 2(b) with $2\ell_b \ell_p N_b N_b^{2\nu}$, we find that all data of fig. 2(b) fall on a universal curve (fig. 5(b))! The scaling implies that for bottle-brush polymers the large values of the effective persistence lengths $\ell_{p,R}$ are entirely due to the side-chain-induced thickening of these flexible cylindrical brushes, at least for the range of side-chain lengths accessible in the simulations. But this range nicely coincides [38] with the range accessible in experiments [9,11,13–15,35,36,39].

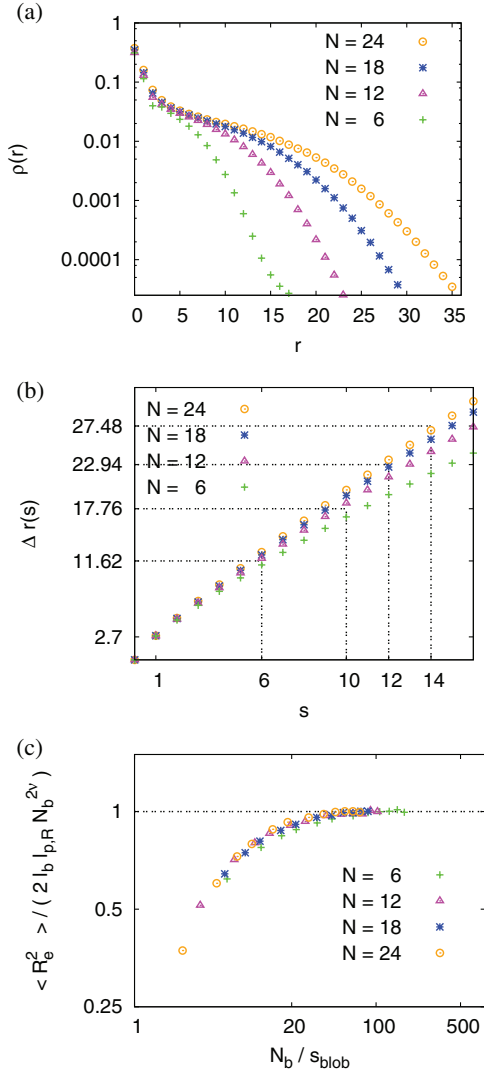


Fig. 5: (Colour on-line) (a) Radial monomer density distribution $\rho(r)$ in planes locally perpendicular to the backbone of bottle-brush polymers with backbone lengths $N_b = 1027$ plotted *vs.* distance r for side-chain lengths $N = 24, 18, 12$ and 6 . (b) Spatial distance $\Delta r(s)$ between monomers a chemical distance s apart plotted on a double-logarithmic scale. The construction $\Delta r(s) = 2R_{cs}(N)$ is shown. (c) Rescaled mean square end-to-end distance of bottle-brush backbones, $\langle R_{e,b}^2 \rangle / (2\ell_b \ell_p N_b^{2\nu})$ plotted *vs.* the rescaled chain length N_b/s_{blob} as described in the text. Note that our length unit (lattice spacing) physically corresponds to about 0.3 nm [38].

Our findings that the persistence length ℓ_p of bottle-brush polymers is of the same order as the cross-sectional radius R_{cs} agrees with the result of Birshtein *et al.* [40] but disagrees with later scaling theories [10,41]. In fact, if $\ell_p \propto R_{cs}$ the second virial coefficient v_2 scales as [28] $v_2 \propto \ell_p^2 R_{cs} \propto \ell_p^3$, and the Flory theory would yield an end-to-end distance [28] $R_e \propto (v_2/\ell_p)^{1/5} \ell_b^{3/5} N_b^{3/5} = \ell_p^{2/5} \ell_b^{3/5} N_b^{3/5}$. A Gaussian behavior, $R_e^2 = \ell_b \ell_p N_b$, is only expected to occur for $\ell_p/\ell_b < N_b/N_b^*$. However, equating the above two expressions for R_e

yields $N_b^* \propto \ell_p/\ell_b$ as well, *i.e.*, in agreement with our findings, the theory of Netz and Andelman [28] also implies that a preasymptotic Gaussian regime does not occur for bottle-brushes. The scaling theories on the contrary imply that $R_{cs} \propto N^{3/4}$ and $\ell_p \propto N^{15/8}$, and hence clearly would predict the existence of a Gaussian regime. Furthermore, even for much larger side-chains the behavior $R_{cs} \propto N^{3/4}$ could not be verified [42]. Although we clearly cannot exclude that the scaling theory might become valid for side-chain lengths of the order of $N \approx 10^3$ or larger, this clearly is completely irrelevant for both experiments [9,11,13–15,35,36,39] and simulations [25,37,38,42]. In fact, self-consistent field calculations [43] have shown that side-chain interactions do have an important effect onto the apparent persistence length only if $N \geq 1000$.

Conclusions. – In summary, we have verified two distinct scenarios for local stiffness of polymer chains: if chain rigidity is caused by an energy term that suppresses chain bending to a large extent, without increase of the cross-sectional radius of the chains, one finds a regime of worm-like chain behavior, described by the Kratky-Porod model (*e.g.*, eq. (3)) for chains up to a chain length N_b^* (where N_b^* can be estimated by a Flory argument, cf. eq. (6) [28]), where a gradual crossover to excluded-volume-dominated behavior (eq. (5)) occurs. However, if chain rigidity is caused by an increase of local chain thickness (as occurs for bottle-brush polymers), no preasymptotic Gaussian regime compatible with the Kratky-Porod model occurs. However, another preasymptotic regime occurs, for $2 < N_b/s_{\text{blob}} < 20$, where $\langle R_{e,b}^2 \rangle$ gradually crosses over from the rod-like behavior $\langle R_{e,b}^2 \rangle \propto N_b^2$, to the excluded-volume behavior, $\langle R_{e,b}^2 \rangle \propto N_b^{2\nu}$ (fig. 5(b)). In a regime where the contour length exceeds the persistence length only a few times, the Kratky-Porod model can be fitted to experimental data, excluded-volume not yet being very important. However, other experiments may fall in a regime where excluded-volume effects are important [44–46]. In [45,46] the importance of excluded volume was inferred from the concentration dependence in semi-dilute solution. Clearly, it is important to carefully examine to which regime experimental data belong.

This work has been supported by the Deutsche Forschungsgemeinschaft (DFG) under grant No. SFB625/A3 and by the European Science Foundation (ESF) under the STIPOMAT program. We thank the Jülich Supercomputing Centre for computer time at the NIC Juropa under the project No. HMZ03 and the SOFTCOMP clusters, and are grateful to S. RATHGEBER, M. SCHMIDT, and A. N. SEMENOV for stimulating discussions.

REFERENCES

- [1] GROSBERG A. YU and KHOKHLOV A. R., *Statistical Physics of Macromolecules* (AIP Press, New York) 1994.
- [2] DES CLOIZEAUX J. and JANNINK G., *Polymers in Solution: Their Modeling and Structure* (Clarendon Press, Oxford) 1990.
- [3] RUBINSTEIN M. and COLBY R. H., *Polymer Physics* (Oxford University Press, Oxford) 2003.
- [4] DE GENNES P. G., *Scaling Concepts in Polymer Physics* (Cornell University Press, Ithaca, NY) 1979.
- [5] SCHÄFER L., *Excluded Volume Effects in Polymer Solutions as Explained by the Renormalization Group* (Springer, Berlin) 1999.
- [6] BUSTAMANTE C., MARKO J. F., SIGGIA E. D. and SMITH S., *Science*, **265** (1994) 1599.
- [7] KÄS J., STREY H., TANG J. X., FINGER D., EZZELL R., SACKMANN E. and JANMEY P. A., *Biophys. J.*, **70** (1996) 609.
- [8] OBER C. K., *Science*, **288** (2000) 448.
- [9] ZHANG M. and MÜLLER A. H. E., *J. Polym. Sci. Part A: Polym. Chem.*, **43** (2005) 3461.
- [10] SUBBOTIN A. V. and SEMENOV A. N., *Polym. Sci. Ser. A*, **49** (2007) 1328.
- [11] SHEIKO S. S., SUMERLIN B. S. and MATYJASZEWSKI K., *Prog. Polym. Sci.*, **33** (2008) 759.
- [12] POTEKIN I. I. and PALYULIN V. V., *Polym. Sci. Ser. A*, **51** (2009) 123.
- [13] WINTERMANTEL M., FISCHER K., GERLE M., RIES R., SCHMIDT M., KAJIWARA K., URAKAWA H. and WATAOKA I., *Angew. Chem., Int. Ed.*, **34** (1995) 1472.
- [14] STEPHAN T., MUTH S. and SCHMIDT M., *Macromolecules*, **35** (2002) 9857.
- [15] LI C., GUNARI N., FISCHER K., JANSHOFF A. and SCHMIDT M., *Angew. Chem., Int. Ed.*, **43** (2004) 1101.
- [16] IOZZO R. V. (Editor), *Proteoglycans: Structure, Biology, and Molecular Interactions* (Marcel Dekker, New York) 2000.
- [17] KLEIN J., *Science*, **323** (2009) 47.
- [18] KRATKY O. and POROD G., *J. Colloid Interface Sci.*, **4** (1949) 35.
- [19] BAWENDI M. G. and FREED K. F., *J. Chem. Phys.*, **83** (1985) 2491.
- [20] LAGOWSKI J. B., NOOLANDI J. and NICKEL B., *J. Chem. Phys.*, **95** (1991) 1266.
- [21] WINKLER R. G., REINEKER P. and HARNAU L., *J. Chem. Phys.*, **101** (1994) 8119.
- [22] STEINHAUSER M. O., SCHNEIDER J. and BLUMEN A., *J. Chem. Phys.*, **130** (2009) 164902.
- [23] SCHÄFER L., OSTENDORF A. and HAGER J., *J. Phys. A: Math. Gen.*, **32** (1999) 7875.
- [24] LE GUILLOU and ZINN-JUSTIN J., *Phys. Rev. B*, **21** (1980) 3976.
- [25] HSU H.-P., PAUL W. and BINDER K., *Macromolecules*, **43** (2010) 3094.
- [26] An analogous hypothesis was suggested for chains at the Theta point, where $\beta = 3/2$ by SHIRVANYANTS D., PANYUKOV S., LIAO Q. and RUBINSTEIN M., *Macromolecules*, **41** (2008) 1475.
- [27] FLORY P. J., *Principles of Polymer Chemistry* (Cornell University Press, Ithaca, NY) 1953.
- [28] NETZ R. R. and ANDELMAN D., *Phys. Rep.*, **380** (2003) 1.
- [29] SCHAEFER D. W., JOANNY J. F. and PINCUS P., *Macromolecules*, **13** (1980) 1280.
- [30] BIRSHTEIN T. M., *Polym. Sci. USSR*, **A24** (1982) 2416.
- [31] BIRSHTEIN T. M. and ZHULINA E. B., *Polymer*, **25** (1984) 1453.
- [32] GRASSBERGER P., *Phys. Rev. E*, **56** (1997) 3682.
- [33] BASTOLLA U. and GRASSBERGER P., *J. Stat. Phys.*, **89** (1997) 1061.
- [34] HOLZER A., *J. Polym. Sci.*, **17** (1955) 432.
- [35] LECOMMANDOUX S., CHIIÉCOT F., BARSALI R., SCHAPACHER M., DEFFIEUX A., BRÛLET A. and COTTON J. P., *Macromolecules*, **35** (2002) 8878.
- [36] ZHANG B., GRÖHN F., PEDERSEN J. S., FISCHER K. and SCHMIDT M., *Macromolecules*, **39** (2006) 8440.
- [37] HSU H.-P., BINDER K. and PAUL W., *Phys. Rev. Lett.*, **103** (2009) 198301.
- [38] HSU H.-P., PAUL W., RATHGEBER S. and BINDER K., *Macromolecules*, **43** (2010) 1592.
- [39] RATHGEBER S., PAKULA T., MATHYJASZEWSKI K. and BEERS K. L., *J. Chem. Phys.*, **122** (2005) 124904.
- [40] BIRSHTEIN T. M., BORISOV O. V., ZHULINA E. B. and YURASOV T. A., *Polym. Sci. USSR*, **29** (1987) 1293.
- [41] FREDRICKSON G. H., *Macromolecules*, **26** (1993) 7214.
- [42] HSU H.-P., PAUL W. and BINDER K., *Macromol. Theory Simul.*, **16** (2007) 660.
- [43] FEUZ L., LEERMAKERS F. A. M., TEXTOR M. and BORISOV O. V., *Macromolecules*, **38** (2005) 8891.
- [44] CHENG G., MELNICHENKO Y. B., WIGNALL G. D., HUA F., HONG K. and MAYS J. W., *Macromolecules*, **41** (2008) 9831.
- [45] BOLISSETTY S., ROSENFELDT S., ROCHETTE C. N., HARNAU L., LINDNER P., XU Y., MÜLLER A. H. E. and BALLAUFF M., *Colloid Polym. Sci.*, **287** (2009) 129.
- [46] BOLISSETTY S., AIRAUD C., XU Y., MÜLLER A. H. E., HARNAU L., ROSENFELDT S., LINDNER P. and BALLAUFF M., *Phys. Rev. E*, **75** (2007) 040803(R).